European Journal of Immunology

Supporting Information

for

DOI 10.1002/eji.201847597

Mathijs Baens, Rocco Stirparo, Youlia Lampi, Delphine Verbeke, Roel Vandepoel, Jan Cools, Peter Marynen, Charles E. de Bock and Simon Bornschein

Malt1 self-cleavage is critical for regulatory T cell homeostasis and anti-tumor immunity in mice

Supplementary Figure 1

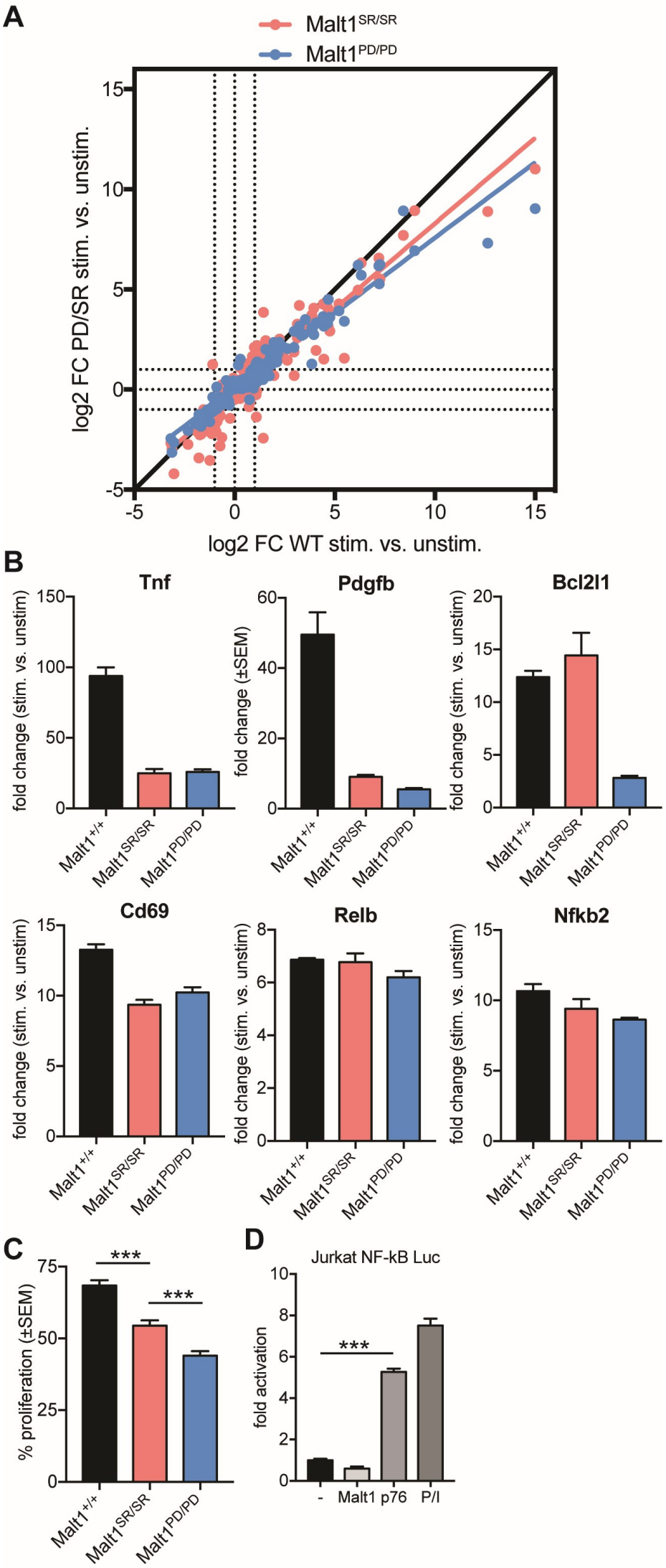

Supplementary Figure 2

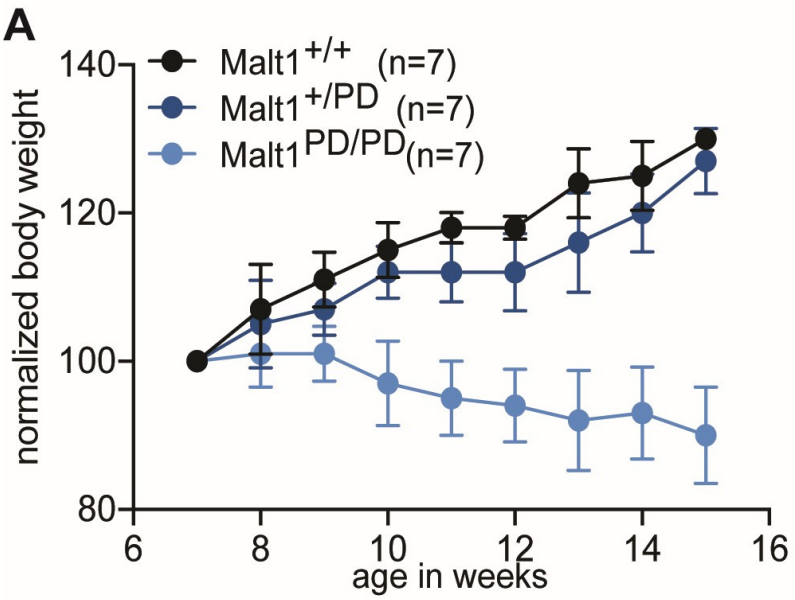

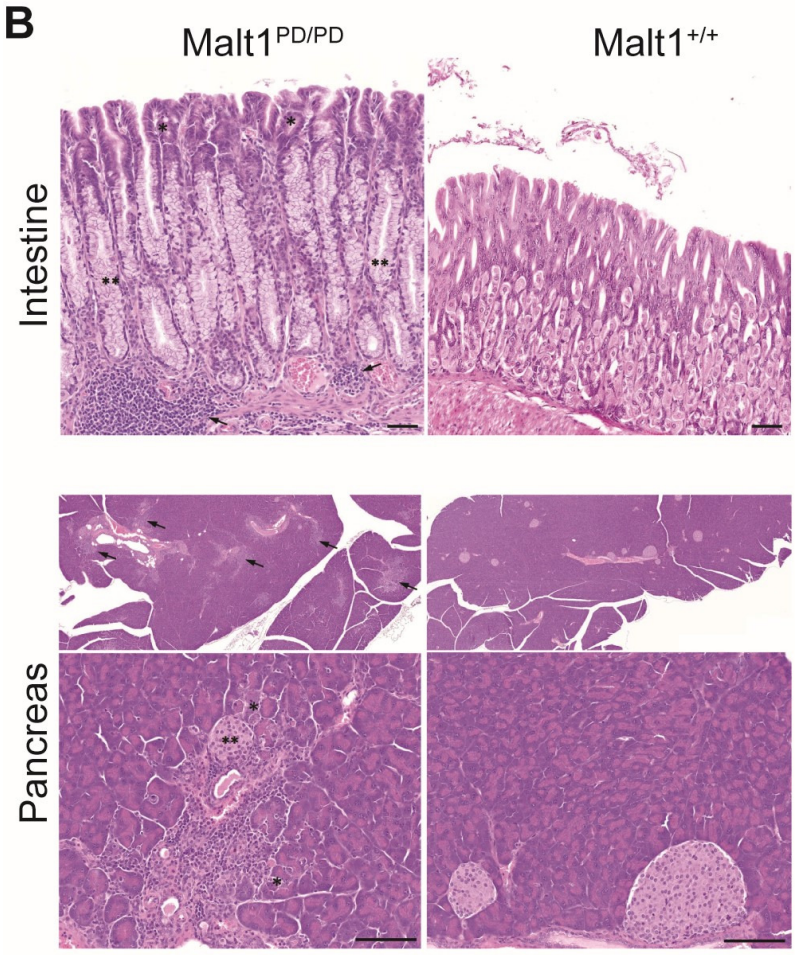

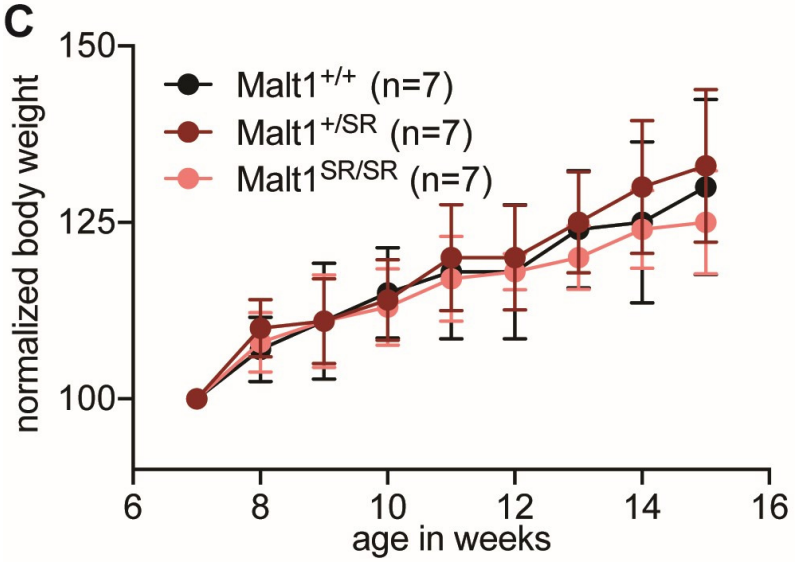

Supplementary Figure 3

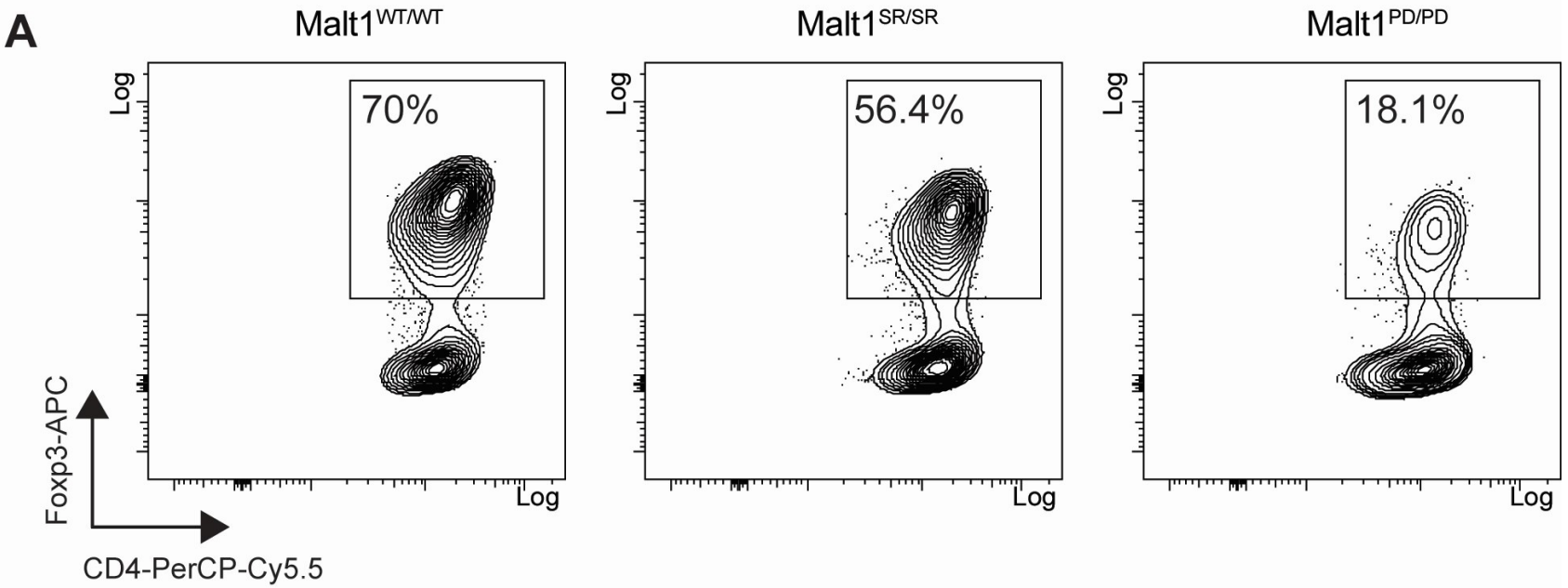

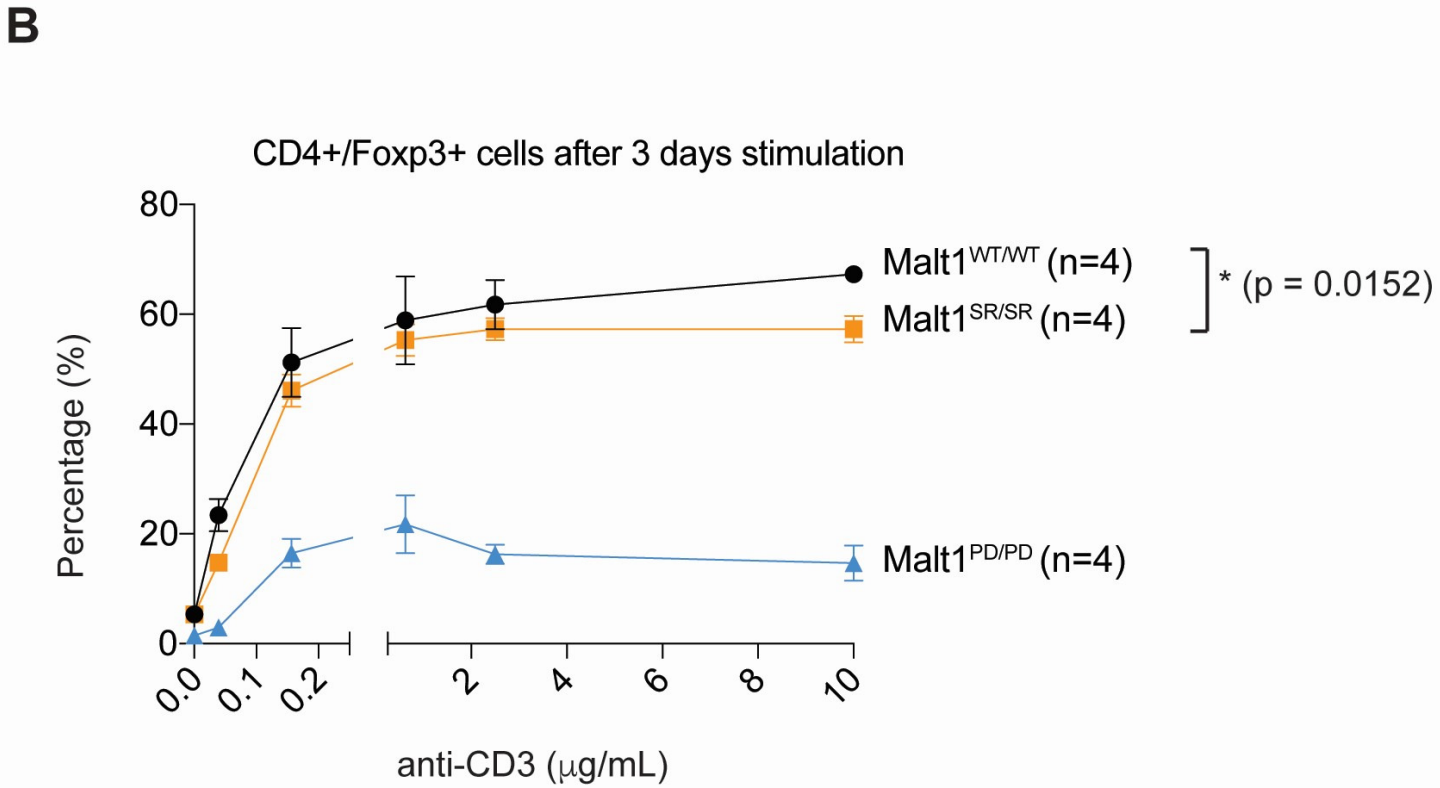

A)

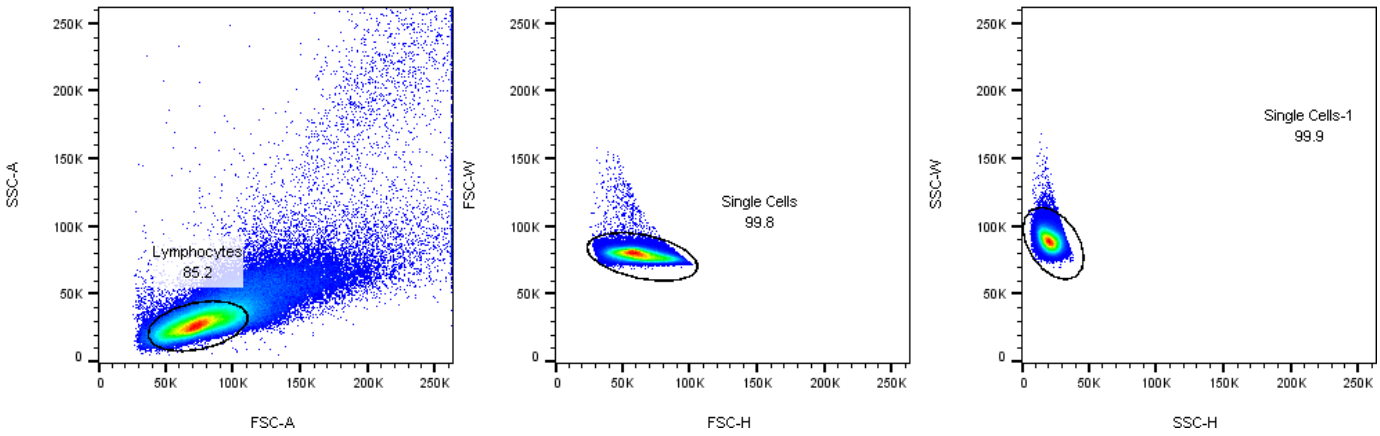
SSC-A
FSC-A
Lymphocytes
85.2
FSC-W
FSC-H
Single Cells
99.8
SSC-W
SSC-H
Single Cells-1
99.9

B)

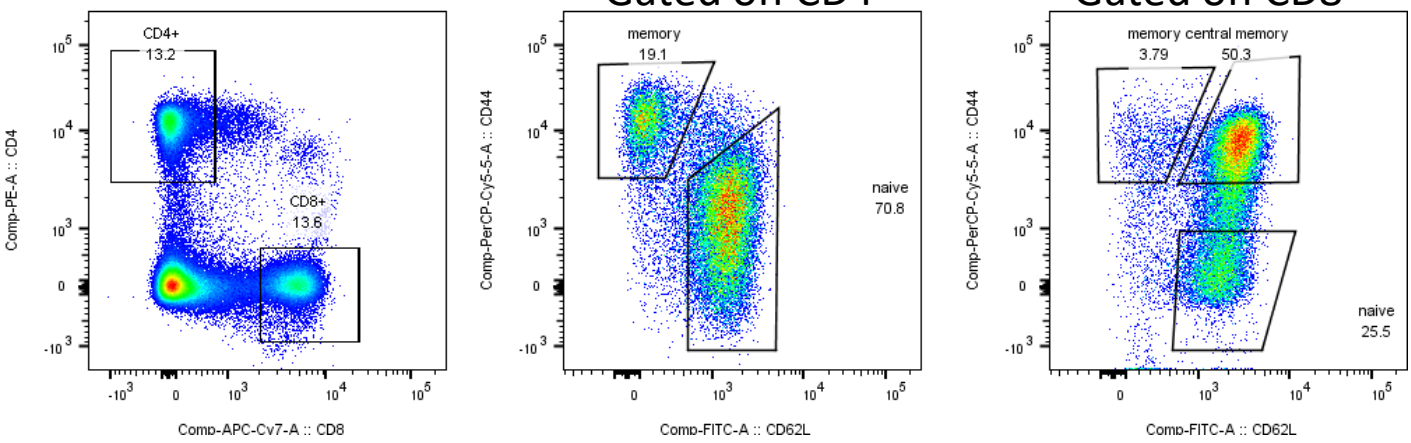
CD4+
13.2
CD8+
13.6
Comp-PE-A :: CD4
Comp-APC-Cv7-A :: CD8
Gated on CD4+
memory
19.1
naive
70.8
Comp-PerCP-Cy5-5-A :: CD44
Comp-FITC-A :: CD62L
Gated on CD8+
memory central memory
3.79
50.3
naive
25.5

C)

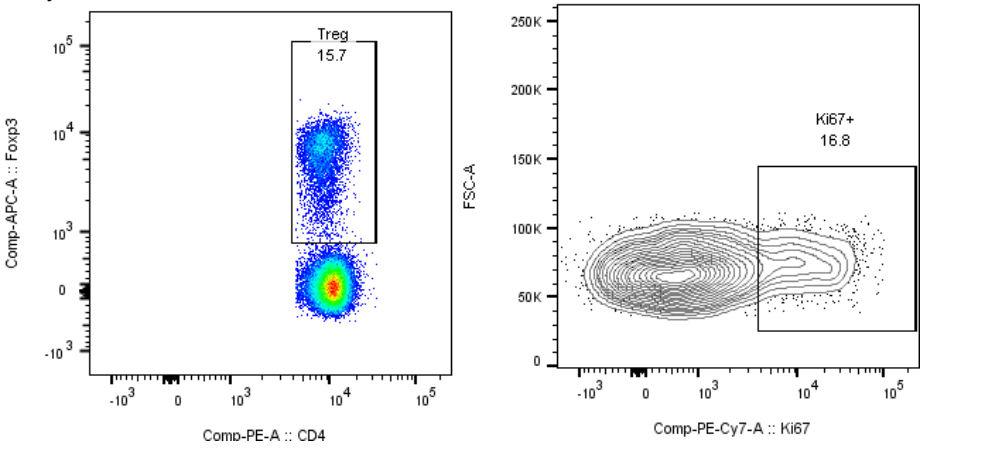
Gated on CD4+
Treg
15.7
Comp-APC-A :: Foxp3
Comp-PE-A :: CD4
Gated on CD4+ Foxp3+
Ki67+
16.8
FSC-A
Comp-PE-Cy7-A :: Ki67

D)

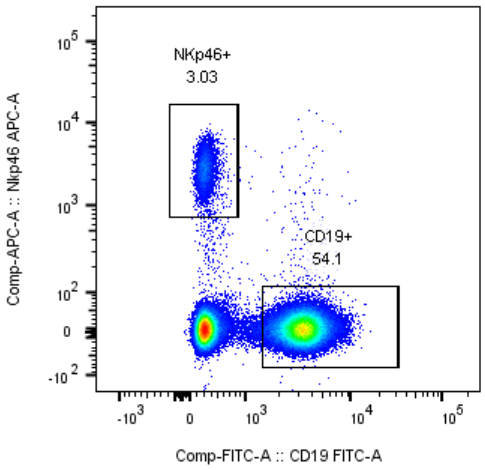

Gated on CD19^{+}

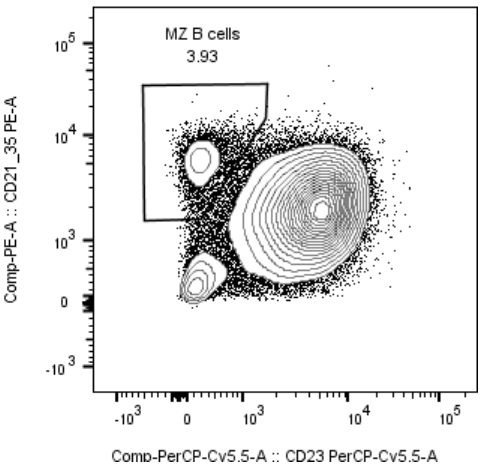

E)

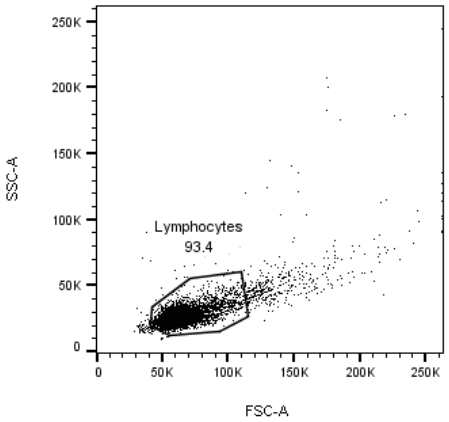

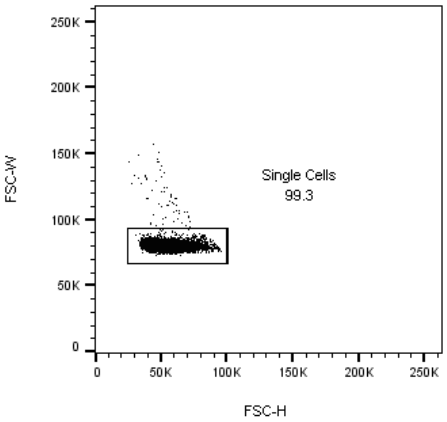

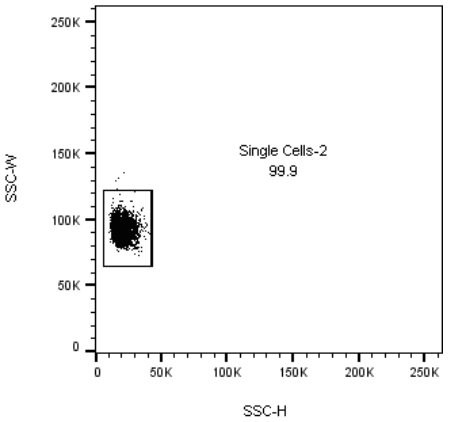

Gated singlets

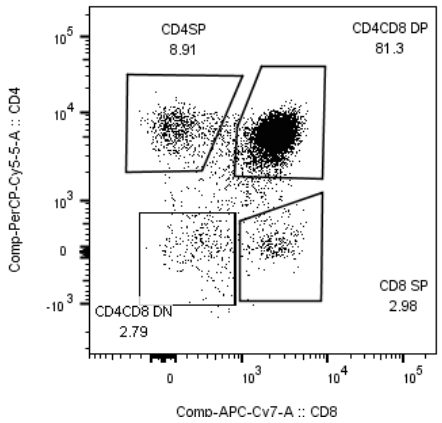

Gated on CD4SP

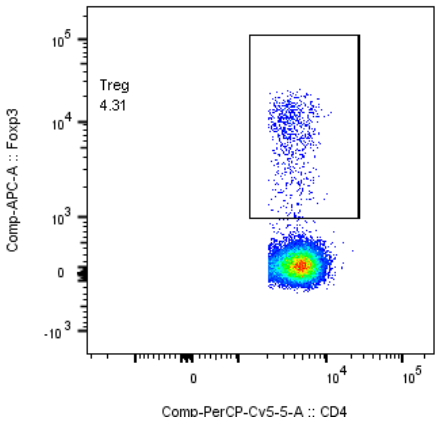

F)

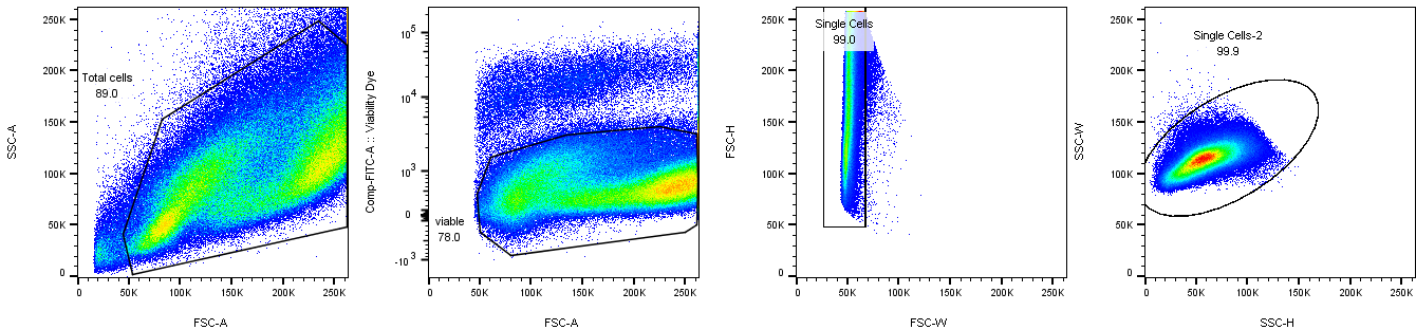

Gated singlets

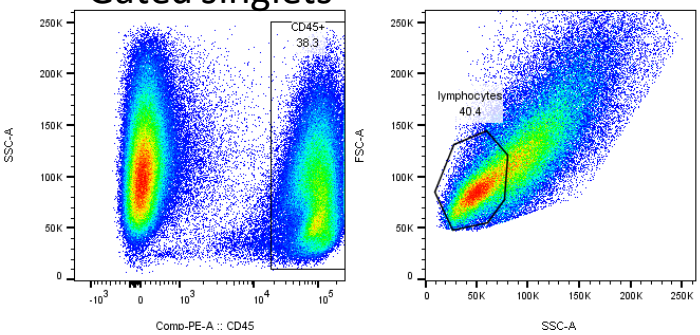

Gated on CD4⁺

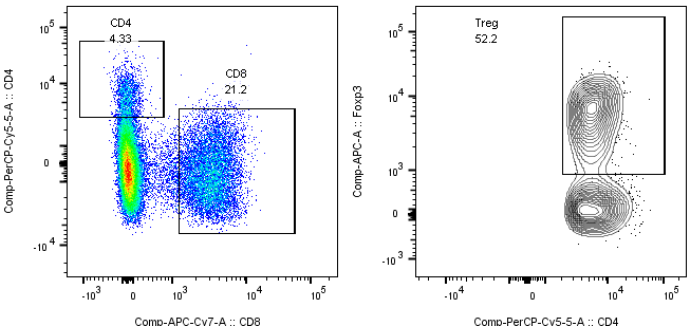

Supplemental Figure Legends

Supplementary Figure 1

(A) RNA-seq data of differential activation of NF-κB target genes (http://www.bu.edu/nf-kb/gene-resources/targetgenes) in unstimulated versus stimulated naïve $CD4^+$ T cells isolated from wild-type ($Malt1^{+/+}$, WT, n=5), self-cleavage resistant ($Malt1^{SR/SR}$, SR, n=4) and protease-dead ($Malt1^{PD/PD}$, PD, n=4) mice. **(B)** Real-time quatitative PCR analysis of the induction of NF-κB target genes, depending on Malt1 protease activity and protease-independent NF-κB target genes (Relb, Nfkb2) in stimulated versus unstimulated naïve $CD4^+$ T cells from different cohorts. ($Malt1^{+/+}$ =3, $Malt1^{SR/SR}$ =3 and $Malt1^{PD/PD}$=3 animals). **(C)** Proliferation of CFSE-labeled naïve CD4 T cells in response to anti-CD3/CD28 stimulation (n=4 animals per group). **(D)** Jurkat cells were electroporated with expression plasmids encoding full-length Malt1 or the self-cleaved Malt1 p76 fragment and an NF-κB luciferase reporter plasmid. As a control Jurkat cells were electroporated with an empty plasmid or stimulated with PMA/ionomycin.

Supplementary Figure 2.

(A) Body weight evolution of $Malt1^{+/+}$, $Malt1^{+/PD}$ and $Malt1^{PD/PD}$ (n=7 per group). Body weights are given normalized to day 7. **(B)** Left top panel, $Malt1^{PD/PD}$ mice. Dense infiltrates of lymphocyte, plasma cells and eosinophils in the deep lamina propria/submucosa (arrows) of the fundic mucosa. Mucosal glands are elongated with prominent expansion of mucus-producing cells and partial to complete loss of parietal and chief cells (**). The architecture of the apical foveolar compartment of fundic glands is maintained (*). Right top panel, $Malt1^{+/+}$ mice. Normal fundic mucosa is shown as comparison. Scale bars = 50μm. Left bottom panels, $Malt1^{PD/PD}$ mice. Pancreas, multiple foci of inflammatory cells (predominantly lymphocytes) infiltrating periductal-perivascular regions (arrows) with loss of adjacent lobuloacinar units (*) and Langerhans islets (**). Right bottom panels, $Malt1^{+/+}$ mice. Normal pancreas sections are

shown as comparison. Scale bars = 100μm. **(C)** Body weight evolution of $Malt1^{+/+}$, $Malt1^{+/SR}$ and $Malt1^{SR/SR}$ (n=7 animals per group). Body weights are given normalized to day 7.

Supplementary Figure 3.

(A) Representative flow cytometry analysis of Foxp3 induction in naïve CD4 T cells at 10 μg/μl anti-CD3, in the presence of TGF-β and Il2. **(B)** Percentage of CD4+/Foxp3+ cells, after three-day stimulation of naïve CD4 T cells in the presence of TGF-β, Il2 and increasing concentrations of plate-bound anti-CD3. Experiment was performed in triplicate with four animals per group.

Supplementary Figure 4.

(A) Example of gating strategy applied for all lymphocyte populations. Gating on FSC-A, SSC-A for lymphocyte selection, followed by gating on single cells. **(B)** Gated on single cells, example of CD4 versus CD8 gating strategy. CD4 gated cells were separated by CD44 and CD62L into naïve ($CD44^-$ $CD62L^+$) and memory ($CD44^+$ $CD62L^-$) subsets. CD8-positive cells were separated by use of CD44 and CD62L into naïve (CD44- CD62L+), central memory ($CD44^+$ $CD62L^+$) and memory ($CD44^+$ $CD62L^-$) subsets. **(C)** Regulatory T cells were identified by gating on $CD4^+$ $CD8^-$ cells, followed by $Foxp3^+$ gating. Regulatory T cells in cell cycle were identified by gating on $Ki67^+$ $CD4^+$ $Foxp3^+$ cells. **(D)** Gated on singlets, NK cells were identified by NKp46 expression and B cells by the expression of cell surface CD19, respectively. Marginal zone (MZ) B cells were identified based on CD21/35 and CD23 staining. **(E)** Thymocyte gating strategy of single cells, and identification of CD4 CD8 double negative (DN), CD4 single positive (SP), CD8SP, and CD4/CD8 double-positive (DP) subsets. Thymic regulatory T cells were defined as CD4SP, Foxp3-positive. (F) Example of gating strategy of MC38 tumor infiltrating lymphocytes. Viable single cells were identified as

displayed and a fixable viability dye was used for live/dead staining. Lymphocytes were identified based on CD45-positivity and size, followed by CD4 CD8 gating. Treg were defined as $CD4^+$ $Foxp3^+$.